Chemical Engineering Journal 163 (2010) 68–77

Contents lists available at ScienceDirect

Chemical Engineering Journal

journal homepage: www.elsevier.com/locate/cej

Biosorption of reactive blue 5G dye onto drying orange bagasse in batch system: Kinetic and equilibrium modeling

Leila D. Fiorentin[a], Daniela E.G. Trigueros[a], Aparecido N. Módenes[b,*], Fernando R. Espinoza-Quiñones[b], Nehemias C. Pereira[a], Sueli T.D. Barros[a], Onélia A.A. Santos[a]

[a] Postgraduate Program of Chemical Engineering, Maringá State University, Av. Colombo 5790, 87020-900 Maringá, PR, Brazil
[b] Postgraduate Program of Chemical Engineering, Paraná West State University, rua da Faculdade 645, Jd. Santa Maria, 85903-000, Toledo, PR Brazil

ARTICLE INFO

Article history:
Received 11 May 2010
Received in revised form 9 July 2010
Accepted 19 July 2010

Keywords:
Biosorption
Orange bagasse
Dye
PSO method
Combined isotherms

ABSTRACT

In this work, orange bagasse has been used as an alternative adsorbent for removal of reactive blue 5G dye from an aqueous solution. The influence of the dye solution pH, the biosorbent drying, the dye solution temperature and biosorbent grain size was studied in batch systems, in order to improve the biosorption kinetics and the experimental equilibrium conditions. Batch kinetic experiments were carried out with different dye concentrations at two temperatures. The biosorption kinetic data were well fitted by both pseudo-first and second order models. The equilibrium adsorption data were interpreted by applying widely the isotherm models and a set of six BET isotherm-added-to other ones and their adjustable parameters were determined by the PSO method. The isotherm models with s-shaped behavior, such as the Langmuir–BET combined isotherm, have described satisfactorily the equilibrium data, suggesting that the dye removal is based on an adsorption process of multi-layers onto the orange bagasse.

1. Introduction

The pollution of water resources with industrial effluents containing organic compounds and toxic substances is a matter of great concern. Generally, waste effluents from textile industries, paper printing and photography contain residues of dyes and chemicals. Synthetic dyes in water bodies, even at very low concentrations, can be highly toxic to living organisms, reducing the growth of bacteria and preventing the photosynthesis in aqueous flora [1,2]. Also, dyes can cause allergy, dermatitis, skin irritation and cancer in humans. Due to the dyes having complex aromatic structures, resistant to light and moderate oxidizing agents, they are usually biologically non-degradable and present high stability and toxicity and it is therefore necessary to eliminate organic pollutants by proper treatment techniques such as adsorption [1–4], electrochemical [5] and membrane processes [6]. The adsorption method is widely used in the removal of synthetic dyes from the industrial effluent [7,8]. By an adsorption process the dye species are transferred to a solid phase (adsorbent) and subsequently can be recovered by a desorption process and stored in a dry place without direct contact with the environment [9–11].

Among the great variety of adsorbents, activated carbon has been widely investigated for organic and inorganic compound removal from waste waters, but the high cost limits its commercial application [12]. Therefore, different types of biomass have been utilized as alternative adsorbent to remove toxic compounds, for example, wheat straw [13], rice straw [14], aquatic plants [15–17], algae [18], sugarcane bagasse [19], banana peel [20] and orange peel [8,21–23].

In addition, orange bagasse is an abundant, cheap and readily available biomass from the orange juice industry. This agricultural by-product creates increasing disposal and potential environmental problems. Based on the various functional groups such as carboxyl and hydroxyl that are found in orange bagasse, this material is proposed as an alternative low-cost adsorbent to remove toxic compounds.

In the present study the use of orange bagasse as biosorbent has been investigated for the reactive 5G dye removal from synthetic textile effluent. Batch kinetic tests were performed in order to assess the effect of dye solution pH, drying temperature, particle size, amount of adsorbent, and contact time. Adsorption kinetic and equilibrium data were modeled by a set of several isotherm models and combined isotherms. The evaluation of kinetic and equilibrium parameters was carried out using the PSO method.

2. Materials and methods

2.1. Materials

A large amount of wet orange bagasse was provided by a local Orange juice industry and used as an alternative low-cost biosor-

* Corresponding author. Tel.: +55 45 3379 7092; fax: +55 45 3379 7002.
E-mail addresses: modenes@unioeste.br, anmodenes@yahoo.com (A.N. Módenes).

1385-8947/$ – see front matter © 2010 Elsevier B.V. All rights reserved.
doi:10.1016/j.cej.2010.07.043

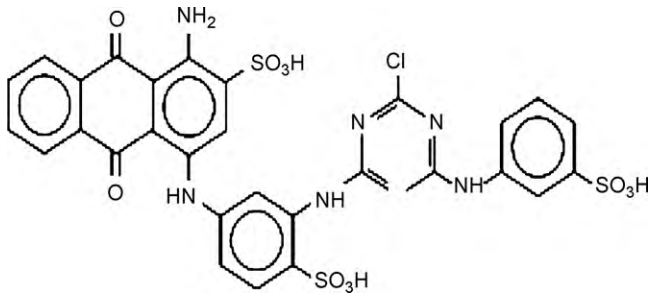

Fig. 1. Chemical structure of reactive blue 5G dye.

bent. After orange juice, essential oils and other sub-products have been extracted, a lot of natural wet orange bagasse was collected and stored below the freezing point (−15 °C) in the laboratory.

The chemicals used were of analytical-reagent grade. Powder of reactive blue 5G dye, whose molecular weight is 840.1 g mol^{-1} and its chemical structure as given in Fig. 1, was diluted in deionized water in order to prepare a set of aqueous solutions, where the initial dye concentration ranged from 25 to 100 mg L^{-1}. Molecular absorbance spectra were measured from diluted pure dyeing solutions in order to identify the maximum absorption wavelength. Before and after any experiment, the solution of the dye concentration was measured using a Shimadzu 1203 UV/VIS spectrophotometer at a 610 nm wavelength. Absorbance data were converted into concentration data by using the calibration relations pre-determined at a 610 nm wavelength for each pH value measured at the end of the experiments. The pH was adjusted by adding 0.1 M H_2SO_4 or 0.1 M NaOH solutions.

2.2. Characterization of the biosorbent

Prior to the nitrogen adsorption experiment to determine surface properties, the orange bagasse samples were defrosted at room temperature and then dried in a convective dryer at low, medium and high settings (42, 66 and 80 °C), under a 1.3 m s^{-1} air flux, until their final weights reached constant values. All samples were ground, using steel-knife electrical mill, and sieved into discrete particle sizes of 0.177, 0.297, and 4.76 mm and stored in closed bottles to be used as adsorbate in the kinetic and adsorption studies.

The BET specific surface area (S_{BET}), average pore diameter (APD), and total pore volume (TPV) of the orange bagasse samples, that were dried at 42, 66 and 80 °C and sieved at 0.177 mm particle size, were determined by the nitrogen adsorption experiments and Barret–Joyner–Halenda (BJH) method. The N_2 adsorption data were measured with a Quantachrome Autosorb-1-C/MS apparatus over a relative pressure ranging from 10^{-6} to 1. S_{BET}, APD and TPV values were obtained by using the software of the apparatus as will be mentioned later in Section 3.1.

SEM high-resolution images of sample surfaces with a 500–2000 magnification range were obtained for orange bagasse-based adsorbents, that were dried at 42, 66 and 80 °C. A Shimadzu superscan SS 550 electron microscope was used for SEM measurements.

2.3. Preliminary tests

In order to improve the kinetic and equilibrium adsorption experimental conditions, the effect of dye solution pH (1–11), particle size (0.177–4.76 mm), and drying temperature (42–80 °C) on the adsorptive removal of reactive 5G dye was investigated in the preliminary batch biosorption experiments. For all the tests, 25 mg of adsorbent material orange bagasse was added to 25 mL of dyeing solution (70 mg L^{-1}) in a 125 mL Erlenmeyer flask, agitated on a rotary shaker at 150 rpm and a 25 °C controlled temperature for 2 h contact time. All preliminary tests were carried out in triplicate. Then the dyeing solution was separated from the biosorbent by using a vacuum filtration system and the dye concentrations were measured spectrophotometrically. The amount of adsorbed dye by orange bagasse was determined according to the mass balance expressed by Eq. (1).

$$q = \frac{V(C_0 - C)}{m} \quad (1)$$

where q (mg g^{-1}) is the amount of adsorbed dye by orange bagasse, C_0 and C are the initial and final dye concentrations in solutions, respectively, V is the solution volume (25 mL), and m is the adsorbent mass (25 mg).

2.4. Kinetic tests

The kinetic data and equilibrium time were determined by using batch studies. Samples consisting of a portion (25 mg) of the adsorbent material orange bagasse (0.177 mm particle size) that was dried at 42 °C and an aqueous solution (25 mL) containing various initial dye concentrations (25–100 mg L^{-1}) at initial pH 2 were poured into 250 mL Erlenmeyer flasks. The samples were agitated on a shaker at 150 rpm and separately at two constant controlled temperatures (25 and 40 °C) up to 48 h contact time. The pH monitoring of the dyeing solution was carried out during the sorption experiments and the pH was adjusted to 2, as required. Samples of the dyeing solution were collected at pre-defined times, ranging from 2 min to 48 h and separated from the adsorbent by using a vacuum filtration system. Dye concentration was measured in each sample by means of UV/vis spectrophotometry and the amount of adsorbed dye by orange bagasse was determined by Eq. (1).

2.5. Equilibrium concentration

Several batch reactive 5G dye sorption experiments with the orange bagasse were carried out using a constant volume of 25 mL solution on different dye concentrations (from 10 to 130 mg L^{-1}) in contact with 25 mg constant biosorbent mass. All equilibrium sorption experiments were carried out in triplicate. The suspensions were agitated by a rotary shaker at 150 rpm and separately at two controlled temperatures (25 and 40 °C), were monitored and adjusted for a pH of 2, during a 2 h contact time. Afterwards, the liquid phase was separated from the suspension using a vacuum filtration system and the initial and equilibrium dye concentrations were measured by means of UV/vis spectrophotometry. The amount of adsorbed dye in the equilibrium condition was determined by Eq. (1).

2.6. Search analysis of kinetic and equilibrium adsorption parameters

The dried orange bagasse-based kinetic and equilibrium biosorption data for reactive blue 5G dye were interpreted on the basis of some models, such as first and second order kinetic rate equations and a set of widely applied adsorption isotherms, as will be mentioned later in Sections 3.4 and 3.5. These equations and isotherms contain two or more kinetic and equilibrium adsorption parameters that are commonly found by means of a linearization method. Generally, the estimated parameters using this method have not shown good fits, because of not taking into account the associated-to-variables error during the search procedure. Nonetheless, search analyses based on non-linear methods have provided a considerable improvement in the results [24]. Generally the optimization methods applied to the estimated adsorption isotherm parameters are very efficient, however they cannot guarantee the best global results, which would converge towards the

best local values, complicating therefore the explanations of the adsorption physics.

In this work, a stochastically optimized global method, called a particle swarm optimization (PSO) proposed by Kennedy and Eberhard [25], has been applied to search for the globally optimized parameter values, which correspond to a set of non-linear models that represent the kinetic and equilibrium adsorption data. The parameter identification procedure based on the PSO method was previously reported by Trigueros et al. [26,27] in order to solve a system of non-linear equations. Trigueros et al. [26,27] have empirically estimated the essential PSO parameter values and their influence on the search space for the estimation of modeling parameters, in order to obtain a quick and good convergence and reliable results.

The description of the PSO algorithm is basically as follows: each individual particle from a swarm population is associated with a position and velocity vectors in the search space, with a dimension equal to the total parameter number of the system, resulting thus that the swarm size equals the particle number. The particle position vector behaves under the restriction of three conditions, that allow delimiting a geographical search space according to a linear vectorial combination, bringing out the particle to assume a new particle position vector [26–28].

Moreover, the minimum and maximum parameter values, which were initially assumed as being those reported in related-to-adsorption literature, were chosen in order to create a first physical constraint in the search space. Based on this assumption, an initial swarm population was generated, avoiding thus results with lesser or without any physical significance. Starting at the swarm lower limit, each particle pathway is calculated in an iterative way, obtaining a new particle position vector [26–28].

According to Trigueros et al. [26,27], the performance of each particle is related to a built-in objective function (OF), determined by the least square statistical method, as shown in Eq. (2) of the present work. When the given iteration number is reached, a better assigned solution, that possesses a set of kinetic parameter values for the modeled system, is used as a new search space constraint on the global minimization process, keeping under control the high sensitivity parameters. Among all visited positions by the swarm, the solution for which the objective function is approached by a minimum value over all the estimated ones is called the best visited position or assigned the best global position. For the PSO method application to kinetic and equilibrium adsorption data, a microcomputer Intel® Core™ 2 Duo 2.0 GHz, with 2 GB RAM memory, was used, where a swarm of 2000 particles with 100 iterations was considered enough to achieve a good convergence, during the search of optimal parameters values.

$$\mathrm{OF} = \sum \left(\frac{q^*_{\mathrm{exp}} - q^*_{\mathrm{pred}}}{q^*_{\mathrm{exp}}} \right)^2 \quad (2)$$

where q^*_{exp} and q^*_{pred} (mg g^{-1}) are the quantities of equilibrium adsorbed dye by orange bagasse, which were experimentally obtained and predictable by modeling, respectively.

3. Results and discussion

3.1. Characterization of adsorbent

The BET-nitrogen specific surface area (S_{BET}) results for dry orange bagasse are listed in Table 1. By employing the Barret–Joyner–Halenda method of calculation, the average pore diameter (APD) and total pore volume (TPV) were also estimated and summarized in Table 1. There is no significant enhancement of S_{BET}, APD and TPV values with an increase of drying temperature.

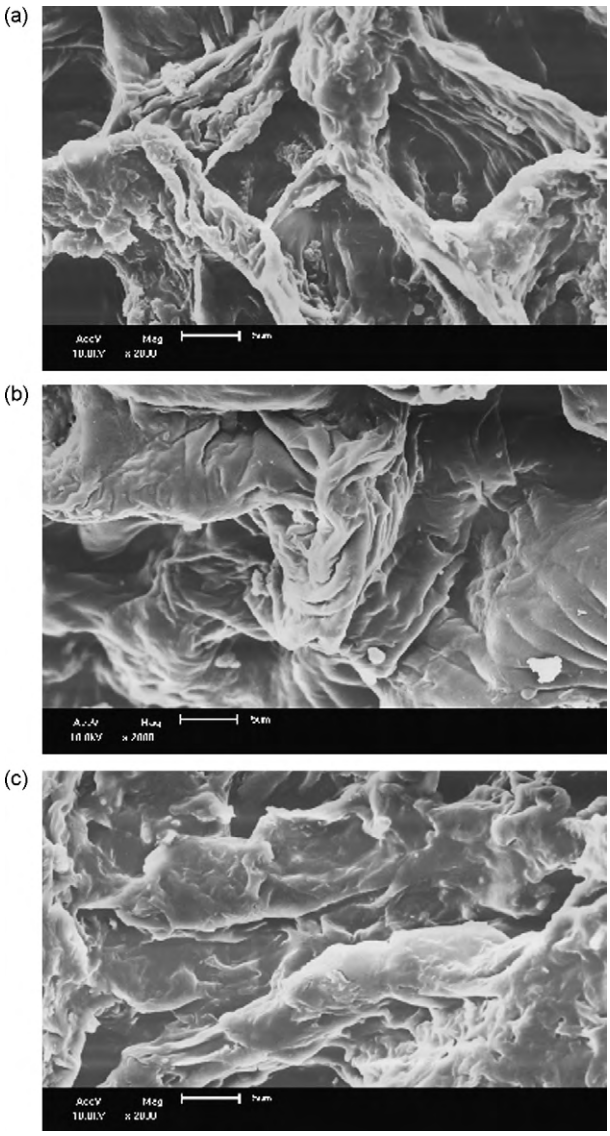

Fig. 2. SEM images for orange bagasse: (a) dried at 42 °C with magnification 2000; (b) dried at 66 °C with magnification 2000; and (c) dried at 80 °C with magnification 2000.

SEM micrographs of drying orange bagasse treated at 42, 60 and 80 °C are shown in Fig. 2. From these images, it is observed that the surface morphology has an irregular pattern within the orange bagasse particle. Consequently, such images did not allow the pore size identification nor the size distribution of the adsorbent or the effect of the drying temperature.

3.2. Effect of pH

In this work the preliminary results on dye adsorption as well as in other works have shown that the pH of the solution is an important controlled parameter. The pH of the dye solution plays an important role in the whole adsorption process that could be influenced not only by the surface charge of the adsorbent, the degree of ionization of the material present in the solution and the dissociation of functional groups in the active sites of the adsorbent, but also the solution of dye chemistry [29]. The influence of pH on the adsorption of reactive 5G dye is shown in Fig. 3. The biosorbent exhibits higher adsorption efficiency, around 85%, of reactive 5G dye at pH 2. This result is not significantly affected by the tested particle size ranges. Consequently, the adsorption

Table 1
Physical characterization of dried orange bagasse determined by BET and BJH methods.

Temperature (°C)	BET specific surface area ($\times 10^{-2}$ m^2 g^{-1})	Total pore volume ($\times 10^{-5}$ cm^3 g^{-1})	Average pore diameter (Å)
42	330.6 ± 3.4	286.4 ± 2.8	21.3 ± 0.8
66	300.7 ± 2.4	278.9 ± 8.0	21.7 ± 1.2
80	297.2 ± 0.7	260.5 ± 1.3	21.1 ± 1.9

capacity increases when the pH is decreasing. So, as dye solution pH decreased, more protons are available in the bulk of the dye solution and the number of negatively charged active sites is reduced, driving the adsorbent surface, which is composed mainly by functional group such as amino and carboxyl, to be more positively charged. Thereby, pH can also affect the structural stability of the reactive blue 5G dye (see Fig. 1). Therein, under an acidic condition, the dye molecule can be deprotonated in the bulk of the solution, resulting in a polar molecule (R-SO_3^-) with a high negative charge density. Therefore, the electrostatic repulsion between the adsorbent site and negatively charged dye ion was lowered at low pH. Consequently, positively charged-functional groups could exert strong electrostatic attractions on anionic dye molecules, explaining thus the increase of the adsorption capacity of the orange bagasse as seen at pH 2 (Fig. 3). Another adsorption mode might be also present (ion exchange or chelation for example). Besides, an abundance of negatively charged surface sites for neutral and alkaline pH values is expected, causing an unfavorable effect on an anionic dye adsorption, because an electrostatic repulsion on surface of the adsorbent is acting, and thus the dye adsorption efficiency drops to 35–48% as shown in Fig. 3.

Similar results were reported for the adsorption of dyes from aqueous solution onto adsorbent prepared from orange peel [30]. Based on the electrostatic attraction, as well the organic properties and structure of the reactive blue 5G dye molecule and orange bagasse, a pH setting at 2 should be used in further adsorption studies to improve the performance of dye removal by an orange bagasse-based biosorbent.

3.3. Effect of particle size and drying temperature

The effects of the drying temperature and the particle size of biosorbent on the adsorption of reactive 5G dye are shown in Fig. 4. It is observed that the adsorption capacity increases when the drying temperature is decreasing, independently of particle size tested. In other words, a high drying temperature of biomass could play a role in a reduction of the number of negatively charged surface sites. On the other hand, for 0.177 mm particle size range a slightly better adsorption capacity was observed than the other two, when the adsorption results of the three particle size ranges were compared (see Fig. 4). Based on the following adsorption conditions: pH 2, drying temperature of 42 °C and particle size below 0.177 mm, a maximum of 88% dye removal was achieved. A low drying temperature (42 °C) and a small particle size (<0.177 mm) should be used in further studies, as well as dye adsorbing of acidic pH.

3.4. Kinetic parameters

The dry orange bagasse-based biosorption kinetic data for a reactive blue 5G dye were determined with the following experimental conditions: pH 2, 25–100 dye concentration range, agitation speed of 150 rpm and both 25 and 40 °C temperatures. As can be seen in Fig. 5, dye removal has increased sharply at contact time less 10 min and slowed down gradually as equilibrium was approached, resulting in an equilibrium time of about 30 min for all the studied cases. Therefore, 30 min of contact time was chosen as the biosorption time for further experiments to ensure that the equilibrium was achieved. In addition, there is no significant influence of dyeing solution temperature over the dye adsorption by orange bagasse, exhibiting a maximum dye removal around 85% for 25 mg L^{-1} dye concentration and a minimum dye removal of about 45% for 100 mg L^{-1} dye concentration. From the literature, on the other hand, an equilibrium time of 60 min was reported by Arami et al. [30] and Alkan et al. [31] using orange peel and sepiolite as biosorbents for the dye removal, respectively.

In order to investigate the mechanism of reactive blue 5G dye adsorption on orange bagasse, two well known differential equations of pseudo first and second orders, called the Lagergren and Ho models, respectively, and intra-particle diffusion equation were proposed in the literature for sorption process [32,33].

Lagergren's first-order equation is the earliest known one describing the adsorption rate based on the adsorption capacity. Besides, Ho's second order date expression, that includes the chemisorption, was successfully applied to the adsorption of metal ions, dyes, herbicides, oils, and organic substances from aqueous

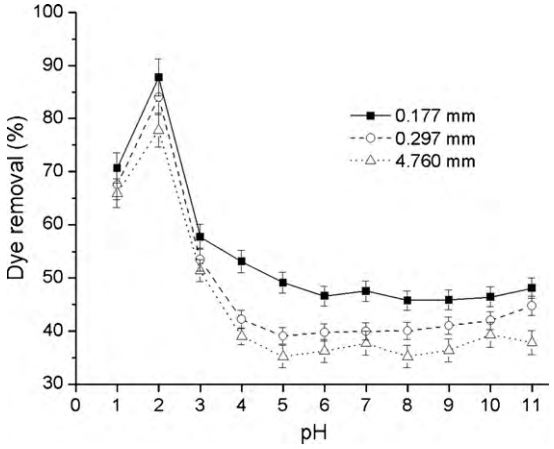

Fig. 3. The effect of equilibrium pH on the adsorption of reactive 5G dye. Conditions: 25 mL dye solution (70 mg L^{-1}), 25 mg biomass (dried at 42 °C), at 150 rpm and 25 °C controlled temperature.

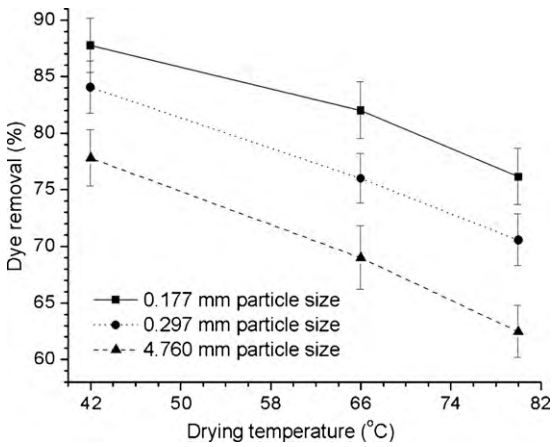

Fig. 4. The effect of drying temperature and particle size on the adsorption of reactive 5G dye. Conditions: pH 2, 25 mL dye solution (70 mg L^{-1}), 25 mg biomass, at 150 rpm and 25 °C controlled temperature.

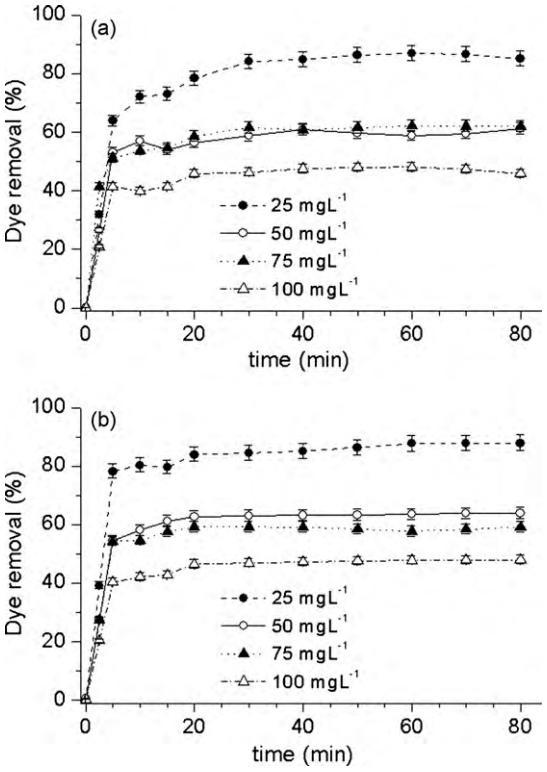

Fig. 5. Kinetic adsorption data of reactive blue 5G dye on orange bagasse at (a) 25 and (b) 40 °C for initial dye concentrations of 25 mg L^{-1} (solid circle), 50 mg L^{-1} (open square), 75 mg L^{-1} (solid triangle up) and 100 mg L^{-1} (open triangle down).

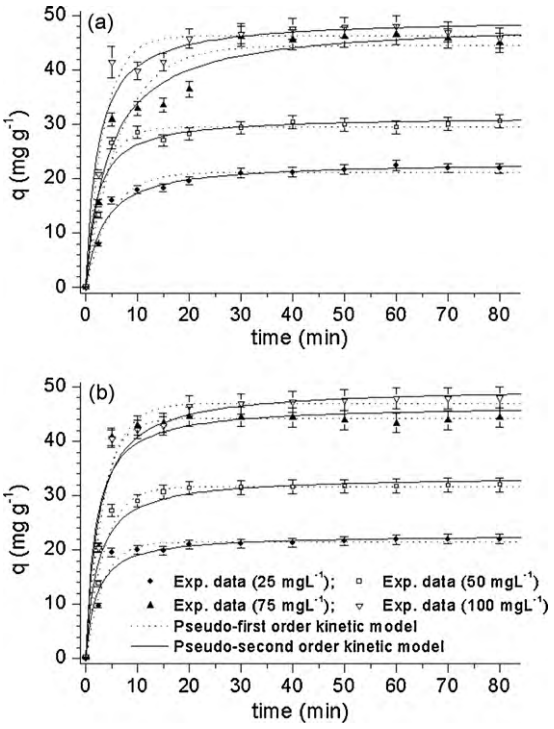

Fig. 6. The fit of the adsorption behavior of reactive blue 5G dye on orange bagasse at (a) 25 and (b) 40 °C for the pseudo first (dot curve) and second (solid curve) order models with initial dye concentrations of 25 mg L^{-1} (solid circle), 50 mg L^{-1} (open square), 75 mg L^{-1} (solid triangle up) and 100 mg L^{-1} (open triangle down).

solutions [34]. Kinetic data of dye adsorption were fitted according to Lagergren and Ho models, which are formulated by Eqs. (3) and (4).

$$\frac{dq}{dt} = k_1(q^* - q) \tag{3}$$

$$\frac{dq}{dt} = k_2(q^* - q)^2 \tag{4}$$

where q^* and q (mg g^{-1}) are the adsorption capacities at equilibrium and at time t (min), respectively, and k_1 (min^{-1}) and k_2 (g mg^{-1} min^{-1}) are the rate constants corresponding to the adsorption of first-order and second order, respectively.

The estimated values of kinetic parameters (q^*_{pred}, k_1 and k_2) corresponding to Lagergren and Ho models were determined by PSO method, as summarized in Tables 2 and 3. Good fits of experimental data for Lagergren and Ho models were achieved in all studied cases, as shown in Fig. 6. It was found that there is a good agreement between adsorption capacity values (q^*_{exp}) at equilibrium and those predicted (q^*_{pred}) by both pseudo first and second order models, with correlation coefficient values ranging from 0.9690 to 0.9919. From the comparison between adsorption capacity values in equilibrium, it was observed that there is no significant improvement in the amount of dye adsorbed onto orange bagasse surface when the dye solution temperature increases from 25 to 40 °C. This result suggests that there are no important factors to be taken into account when the reactor conditions are chosen within an adsorption system for dye removal.

On the other hand, the possibility of intra-particle diffusion being the rate-limiting step was also investigated in the orange bagasse-based dye adsorption system. According to the intra-particle diffusion model proposed by Weber and Morris [35], the root time dependence may be expressed by Eq. (5). Weber and Morris stated that if intra-particle diffusion is the rate-controlling factor, uptake of the adsorbate varies with the square root of time.

$$q_t = k_{dif}\sqrt{t} + C \tag{5}$$

where q_t is the amount of solute on the adsorbent surface at time t (mg g^{-1}), k_{dif} the intra-particle diffusion rate constant (mg g^{-1} $min^{-1/2}$), t the time (min), and c is the intercept (mg g^{-1}).

So, the kinetic data at different initial dye concentrations can be used to determine if intra-particle diffusion is rate-limited factor in the dye adsorption process on orange bagasse, then plots of adsorbate uptake (q_t) versus the square root of time ($t^{1/2}$) would result in a linear relationship and k_{dif} and C values can be obtained from these plots (Fig. 7) and Table 4. Values of the intercept give an idea about the thickness of the boundary layer. Fig. 7 shows that all Weber–Morris plots of dry orange bagasse for intra-particle transport are not linear over the whole $t^{1/2}$ range and can be separated into a few linear regions, revealing that there are two or three adsorption stages with different slopes taking place. It can be observed that there are three separate regions at low dye solution temperature (25 °C) for the whole of 25–100 mg L^{-1} initial dye concentration range, while they are observed only at high dye solution temperature (40 °C) with initial dye concentration above 50 mg L^{-1}.

Usually, the initial curved portion is attributed to external surface adsorption that the adsorbate diffuses through the solution to the external surface of the adsorbent, where the adsorption rate is high. The second portion is attributed to the macro-pore diffusion, considered as the gradual adsorption stage, where the intra-particle diffusion is rate-controlled step on adsorbent. Moreover, the particle diffusion would be the rate-controlling step if the lines passed through the origin. Finally, the plateau (third region) is attributed to micro-pore diffusion, considered as the equilibrium stage, in which the intra-particle diffusion starts to slow down and level out as the extremely low dye concentration remains in the solution or maximum adsorption was attained. In the gradual adsorption stage (see Fig. 7), the diffusion rate parameters k_{dif} obtained from the slopes

Table 2
Kinetic adsorption data for experimental conditions: pH 2, 0.177 particle size and 25 °C temperature adsorption and parameter values predicted by PSO method for pseudo first and second order models.

C_0 (mg L^{-1})	q^*_{exp} (mg g^{-1})	Lagergren model				Ho model			
		k_1 (min^{-1})	q^*_{pred} (mg g^{-1})	OF[a]	R^2	k_2 (g mg^{-1} min^{-1})	q^*_{pred} (mg g^{-1})	OF[a]	R^2
25	21.0199	0.2124	21.2108	14.0934	0.9860	0.0129	23.1161	9.3967	0.9908
50	29.3532	0.3106	29.5801	26.7983	0.9857	0.0160	31.4661	41.7916	0.9776
75	46.1443	0.1523	44.4829	146.9976	0.9690	0.0046	48.9190	79.5432	0.9828
100	46.6501	0.2912	46.3441	87.3318	0.9809	0.0093	49.4956	93.2152	0.9796

[a] OF is the objective function estimated by Eq. (2).

Table 3
Kinetic adsorption data for experimental conditions: pH 2, 0.177 particle size and 40 °C temperature adsorption and parameter values predicted by PSO method for pseudo first and second order models.

C_0 (mg L^{-1})	q^*_{exp} (mg g^{-1})	Lagergren model				Ho model			
		k_1 (min^{-1})	q^*_{pred} (mg g^{-1})	OF[a]	R^2	k_2 (g mg^{-1} min^{-1})	q^*_{pred} (mg g^{-1})	OF[a]	R^2
25	21.1194	0.3156	21.4619	13.1550	0.9865	0.0220	22.7599	20.6850	0.9786
50	31.4676	0.2853	31.6510	17.2454	0.9919	0.0137	33.5789	39.1555	0.9814
75	44.4495	0.3311	44.2186	46.6582	0.9888	0.0121	46.6167	112.7089	0.9723
100	46.8750	0.0088	49.9570	76.8486	0.9838	0.2796	47.1942	55.4750	0.9883

[a] OF is the objective function estimated by Eq. (2).

of straight lines (see Table 4) vary with the initial dye concentrations (25–100 mg L^{-1}) and dye solution temperatures (25 and 40 °C); however, none of the lines passed through the origin according to the non-zero values of intercept parameters C, indicating that there is an initial boundary layer resistance, i.e., the intra-particle diffusion is involved but not as the only rate-controlling step.

From the best-fit straight lines on the gradual adsorption stage (Fig. 7), it was found that both the C and k_{dif}, values (see Table 4) increase with the increasing of the initial dye concentration, suggesting an increase in the thickness and the effect of the boundary layer. Similar results were reported for the adsorption of basic dye onto zeolite MCM-22 [36], acid dye adsorption on activated palm ash [37], basic Green 4 onto cyclodextrin-based adsorbent [29], and Congo red onto clay materials [2]. Besides, it was also observed that there is a dye solution temperature effect on the values of diffusion rate constants k_{dif}, driving it to lower values when the dye solution temperature is increased, which suggests a decrease in the thickness and the effect of the boundary layer with the increase of the dye solution temperature.

3.5. Equilibrium adsorption parameters

Adsorption isotherms of dyes were determined on the basis of batch analysis with the following experimental conditions: pH 2, agitation speed of 150 rpm, 25 and 40 °C temperatures used in a series of dye solutions at various concentrations, ranging from10 to 130 mg L^{-1}. These isotherms represent an equilibrium relation between dye concentrations in fluid phase and the amount of dye with a bioadsorbent mass for a specific temperature. The isotherm is very important in order to estimate the maximum adsorption capacity and affinity between adsorbate and adsorbent, besides other physical parameters. Since the adsorption phenomenon response is related to the kind of material used for the adsorbent and the chemical and physical characteristics possessed by the adsorbate, as well as the adsorption experimental conditions, a number of adsorption processes for pollutants have been studied in an attempt to find a suitable explanation for the mechanisms and kinetics for sorting out the environmental solutions [35].

As a first attempt to reproduce the dye adsorption data, well-known and widely applied isotherm models of Langmuir and Freundlich, as well as the BET isotherms, were applied, as summarized in Table 5 and their adsorption parameters were estimated by the PSO method. Experimental isotherm data for both 25 and 40 °C temperatures are given in Fig. 8 where the fitted Langmuir, Freundlich and BET isotherm curves are also shown. The first part of the equilibrium adsorption data, below 80 mg L^{-1} dye concentration, has been roughly fitted by both Langmuir and Freundlich isotherm models. However, the s-shaped behavior of equilibrium adsorption data was not reproduced by both Langmuir and Freundlich isotherms; but the BET isotherm curve reproduces well the sigmoidal tendency of the dye adsorption experimental points. This sigmoidal behavior might be interpreted as a change of the mechanism in a dye adsorption process. Dye is initially adsorbed onto the first layer of biosorbent surface at low dye concentration; but when it has reached its saturation (about 80 mg L^{-1} dye concentration), another biosorption phenomenon begins to become evident by mean of a dye adsorption process onto the multi-layer orange bagasse surface. By examining the goodness of fit of kinetic models with experimental data, the predicted results by BET isotherm model were almost in full agreement with the experimental data at

Table 4
Intra-particle diffusion model parameters (k_{dif} and C) for different initial reactive blue 5G dye concentrations at 25 and 40 °C.

Solution temperature (°C)	C_0 (mg L^{-1})	k_{dif} (mg g^{-1} min$^{-1/2}$)	C (mg g^{-1})	R^2
25	25	1.51	12.77	0.9739
	50	3.31	14.20	0.8540
	75	4.45	18.87	0.8316
	100	6.08	18.73	0.9531
40	25	0.52	18.34	0.8330
	50	1.38	24.65	0.8836
	75	1.14	38.82	0.8670
	100	2.17	35.40	0.9043

Table 5
Isotherm models used to form combined isotherms by addition, the BET isotherm is part of them.

Isotherm	Expression	Application	Characteristic
Langmuir	$q^* = \frac{q_{max} bC^*}{1+bC^*}$	Mono layer homogeneous surfaces	Two theoretical parameters
Freundlich	$q^* = K_F(C^*)^{1/n}$	Multi-layer heterogeneous surfaces	Two empirical parameters
Sips	$q^* = \frac{K_S(C^*)^{\beta_S}}{1+a_S(C^*)^{\beta_S}}$	Combined Langmuir–Freundlich	Three semi-empirical parameters
Redlich–Paterson	$q^* = \frac{K_{RP}C^*}{1+a_{RP}C^{*n}}$	Heterogeneous surfaces	Three semi-empirical parameters
Radke–Praunsnitz	$q^* = \frac{q_{max} bC^*}{(1+bC^*)^n}$		Three empirical parameters
Toth	$q^* = \frac{q_{max} bC^*}{(1+b(C^*)^n)^{1/n}}$	Multi-layer heterogeneous surfaces	Three empirical parameters
Temkin	$q^* = \frac{RT}{b_T} \ln(a_T C^*)$	Mono layer chemisorption	Two theoretical parameters
BET	$q^* = \frac{q_{max} BC^*}{(C_S - C^*)[1+(B-1)(C^*/C_S)]}$	Multi-layer physisorption	Two theoretical parameters

Table 6
Equilibrium adsorption parameters predicted by PSO method for BET isotherm model.

Temperature (°C)	q_{max} (mg g^{-1})	B	C_S (mg L^{-1})	OF	r^2
25	25.9846	49.1137	165.4738	0.0687	0.9909
40	28.90	31.1450	189.2222	0.1177	0.9788

all dye concentrations, with correlation coefficient values of 0.9909 (objective function value of 0.0687) and 0.9788 (objective function value of 0.1177) for 25 and 40 °C temperatures, respectively. The BET isotherm parameters for the dye adsorption studied on the orange bagasse are given in Table 6. Thus, the s-shaped behavior that was observed on equilibrium adsorption data is probably a sign of the change of mechanism in adsorption process from mono- to multi-layers on the material surface at a specific equilibrium concentration, suggesting that there is a reduction in the availability of active sites when the dyeing solution concentration is increasing.

New combined isotherm models were built by an addition of a widely applied isotherm model, such as Langmuir, Freundlich, Sips, Redlich–Patterson, Radke–Praunsnitz, Toth and Temkin, to a BET isotherm, in order to understand better the sigmoidal behavior of experimental adsorption data, which deserve very thorough elucidation. A set of combined isotherms (BET isotherm added to other ones) were applied for the whole 0–120 mg L^{-1} dye concentration range. Good fits of experimental data were obtained (see Fig. 9) by applying built-in isotherm models based on the BET isotherm. Adjustable parameters corresponding to combined isotherm models were also estimated by the PSO method and their values and indicators of the goodness of fit (objective function and correlation

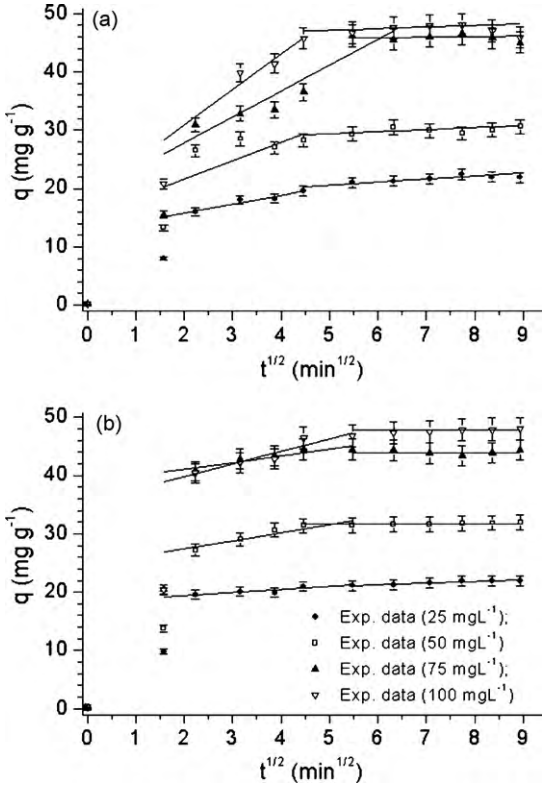

Fig. 7. Intra-particle kinetic diffusion for adsorption of the reactive blue 5G dye on orange bagasse at initial pH 2 and two dye solution temperatures: (a) 25 and (b) 40 °C with initial dye concentrations of 25 mg L^{-1} (solid circle), 50 mg L^{-1} (open square), 75 mg L^{-1} (solid triangle up) and 100 mg L^{-1} (open triangle down).

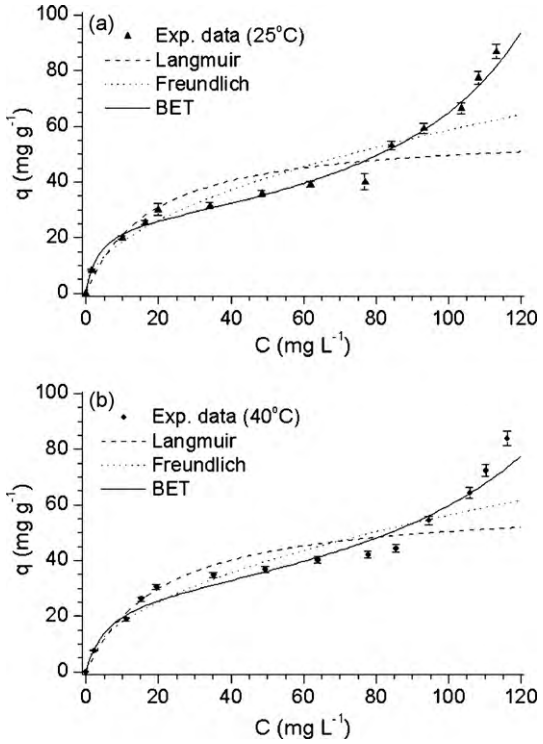

Fig. 8. The fit of the experimental adsorption data at (a) 25 °C (solid triangle up) and (b) 40 °C (solid circle) for Langmuir (dash curve), Freundlich (dot curve), and BET (solid curve) isotherm models with reactive blue 5B dye, using orange bagasse as biosorbent.

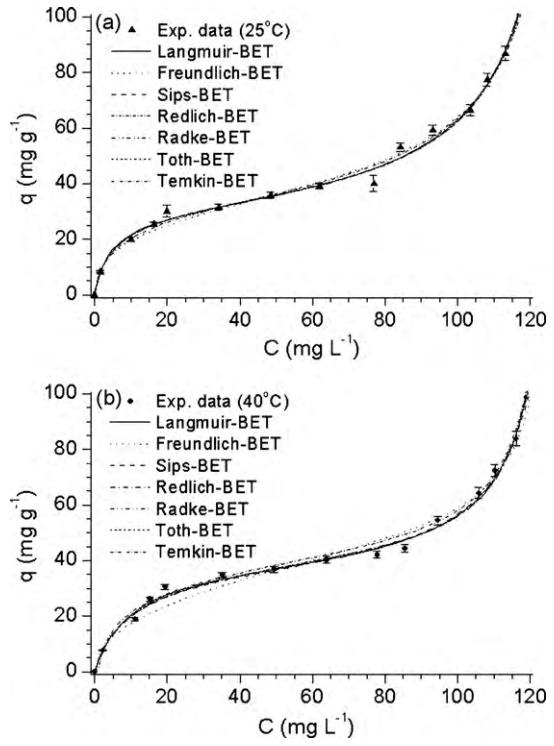

Fig. 9. The fit of the experimental adsorption data at (a) 25 °C (solid triangle up) and (b) 40 °C (solid circle) with Langmuir–BET (solid curve), Freundlich–BET (dot curve), Sips–BET (dash curve), Redlich–BET (dash-dot curve), Radke–BET (dash-dot-dot curve), Toth–BET (short dash curve), Temkin–BET (short dash dot) isotherm models for reactive blue 5B dye, using orange bagasse as biosorbent.

coefficient) are summarized in Table 7, where q_{max1} is the maximum adsorption capacity for the isotherm added to the BET one and q_{max2} is the maximum adsorption capacity for the BET isotherm.

Combined isotherm models, that were built by the addition of an empirical isotherm (Sips, Redlich–Paterson, Radke–Prausnitz and Toth) to the BET isotherm, have shown good agreement with the dye adsorption experimental points, following their sigmoidal tendency and have given the same response as shown by the Langmuir–BET isotherm model.

The results obtained, from the fits of BET and combined isotherm models to dye adsorption experimental points, suggest that the dye adsorption continues beyond the first layer, from which there is a significant vertical interaction between the adsorbed molecules, resulting in overlapping multi-layer adsorption. In this case, the ability of molecules to fix onto the surface of the adsorbent depends on the occupation of neighboring active sites. Applying the Langmuir–BET isotherm model, the first layer could be characterized and quantified by the first isotherm based on the adsorption by a mono-layer as the Langmuir one, while the characterization of subsequent layers could be obtained by the combined isotherm (BET isotherm).

The formation of the saturated first layer is characterized by the appearance of the inflection point in the equilibrium data, which can be quantified by the B-parameter value of the BET isotherm. Applying the BET isotherm model, the B-parameter value (see Table 6) suggests that adsorbent–adsorbate positive interactions are larger in the first layer (B = 49.11 at 25 °C), while for the combined isotherms, B-parameter values decrease in the subsequent layers, ranging from 9.77 to 39.87 at 25 °C (see Table 7). Moreover, it is observed that there is a decrease of the maximum dye adsorption capacity values, corresponding to the first layer (15.58–24.23 mg g^{-1} q_{max1} value range for first isotherm) as compared to subsequent layers (9.97–11.81 mg g^{-1} q_{max2} value range

Table 7
The estimated parameter values for the combined isotherms at temperatures of 25 and 40 ± 1 °C and pH 2.

Combined model	Temperature (°C)	Parameters													OF	R^2
		q_{max} (mg g^{-1})	b (L mg^{-1})	K_F (L g^{-1})	n	a_T (L g^{-1})	b_T (kJ mol^{-1})	K_S (L g^{-1})	a_S (L mg^{-1})	β_S	K_{RP} (L g^{-1})	a_{RP} (L mg^{-1})	q_{max} (mg g^{-1})	B	C_S (mg L^{-1})	
Langmuir–BET	25	21.11	0.3140										11.8175	9.77	136.77	0.0444	0.9944
	40	33.2836	0.0997										6.2642	15	130.9834	0.0462	0.9952
Freundlich–BET	25			5	2.5608								8.6290	39.8740	134.00	0.0775	0.9926
	40			5	2.1519								3.7854	25.9272	129.3802	0.1499	0.9863
Sips–BET	25	24.2345	0.20		1.2390			4.8469	0.20	0.8071			10.6571	12.8751	134.7272	0.0428	0.9942
	40	34	0.0899		1.10			3.0566	0.0899	0.9090			6.6965	13.2225	132.2550	0.0478	0.9951
Redlich–Paterson–BET	25	15.5830	0.4704		0.90						7.3302	0.4704	9.9678	14.6817	133.8140	0.0444	0.9940
	40	24.0399	0.1642		0.90						3.9473	0.1642	4.7925	14.2328	128.3712	0.0496	0.9939
Radke–Prausnitz–BET	25	16.3790	0.4107		0.90								10.3091	14	134.4008	0.0446	0.9940
	40	27.7838	0.1297		0.90								5.1646	14.8327	129.0720	0.0486	0.9943
Toth–BET	25	19.4636	0.4477		0.7493								10.3218	10	134.1753	0.0433	0.9941
	40	23.6917	0.1716		0.75								4.9474	20	128.5870	0.0488	0.9939
Temkin–BET	25					3.2405	0.5858						10.8065	11.5088	136.6157	0.0526	0.9938
	40					1.0948	0.3314						4.8381	11.3584	128.6687	0.0458	0.9821

Sips isotherm: $K_S = q_{max}b$; $\beta_S = 1/n$ and $a_S = b$; Redlich–Paterson isotherm: $K_{RP} = q_{max}b$ and $a_{RP} = b$; q_{max2} is q_{max} for BET isotherm.

for BET isotherm). In addition, with a rising temperature an increase in q_{max1} values was observed and consequently a reduction in q_{max2} values, resulting in an insignificant influence of temperature on the total adsorption capacity. The total contribution of all layers on the maximum dye adsorption capacity could be calculated by the addition of q_{max1} and q_{max2} values. Therefore, the maximum dye adsorption capacity values were ranging from 25.55 to 34.89 mg g^{-1} at 25 °C and from 28.64 to 40.70 mg g^{-1} at 40 °C for all the saturated layers. All evaluated models predict that saturation occurs at a dye concentration of about 134 and 132 mg L^{-1} at 25 and 40 °C, respectively.

Thus, from the study of equilibrium adsorption of the reactive blue 5G dye on orange bagasse it can be assumed that the isotherms with sigmoid behavior, such as the Langmuir–BET combined isotherm have described satisfactorily the equilibrium data, characterizing and quantifying the phenomenon adequately.

4. Conclusion

The results of this study indicate that the orange bagasse shows a significant capacity to adsorb the reactive blue 5G dye. Batch tests revealed that the best conditions for adsorption of reactive blue 5G dye occur at pH 2 and dried orange bagasse at the temperature of 42 °C. At this temperature the particle size has no significant influence on the removal of the dye, and therefore particles with average diameter of 0170 mm can be successfully used. At acidic pH a high electrostatic attraction exists between the positively charged surface of the adsorbent and the anionic dye.The equilibrium and kinetic study showed that the solution temperature does not exert significant influence on the removal of reactive blue 5G dye by orange bagasse. The adsorption equilibrium time was achieved in 30 min for concentrations of 25, 50, 75 and 100 mg L^{-1} and temperatures of 25 and 40 °C. Moreover, the kinetic tests showed that in only 5 min contact the dye removal was above 80%, suggesting a high percentage of the initial removal of the synthetic pollutant. Both models pseudo-first order and pseudo-second order fit satisfactorily the kinetic data obtained for the solution temperatures of 25 and 40 °C. It was also observed that intra-particle diffusion is involved in the sorption process.The equilibrium data of adsorption of synthetic dye solution at temperatures of 25 and 40 °C showed a sigmoidal isotherm behavior, which were adequately correlated by applying combined isotherms, suggesting a multilayer adsorption. In the first layer the maximum dye adsorption capacity was estimated at 15.58–24.23 mg g^{-1} (23.69–34 mg g^{-1}) and in all saturated layers it was estimated at 25.55–34.89 mg g^{-1} (28.64–40.70 mg g^{-1}) for 25 °C (40 °C).

Nevertheless, due to its good characteristics for dye removal such as low equilibrium time, quick dye removal rate, and maximal dye uptake, the orange bagasse can be considered as alternative biosorbent toward the implementation of biosorption technology in industrial and environmental remediation.

Acknowledgements

Leila D. Fiorentin and D.E.G. Trigueros thank to the Brazilian research supporting agencies - CNPq and CAPES for Ph.D. scholarship, respectively.

References

[1] B.H. Hameed, Equilibrium and kinetic studies of methyl violet sorption by agricultural waste, J. Hazard. Mater. 154 (2008) 204–212.
[2] V. Vimonses, S. Lei, B. Jin, C.W.K. Chow, C. Saint, Kinetic study and equilibrium isotherm analysis of Congo Red adsorption by clay materials, Chem. Eng. J. 148 (2009) 354–364.
[3] M. Arami, N.Y. Limaee, N.M. Mahmoodi, Evaluation of the adsorption kinetics and equilibrium for the potential removal of acid dyes using a biosorbent, Chem. Eng. J. 139 (2008) 2–10.
[4] F. Batzias, D. Sidiras, E. Schroeder, C. Weber, Simulation of dye adsorption on hydrolyzed wheat straw in batch and fixed-bed systems, Chem. Eng. J. 148 (2009) 459–472.
[5] S.M. Palácio, F.R. Espinoza-Quiñones, A.N. Módenes, C.C. Oliveira, F.H. Borba, F.G. Silva Jr., Toxicity assessment from electro-coagulation treated-textile dye wastewaters by bioassays, J. Hazard. Mater. 172 (2009) 330–337.
[6] S.N. Su, H.L. Nie, L.M. Zhu, T.X. Chen, Optimization of adsorption conditions of papain on dye affinity membrane using response surface methodology, Bioresour. Technol. 100 (2009) 2336–2340.
[7] T. Calvete, E.C. Lima, N.F. Cardoso, S.L.P. Dias, F.A. Pavan, Application of carbon adsorbents prepared from the Brazilian pine-fruit-shell for the removal of Procion Red MX 3B from aqueous solution—kinetic, equilibrium, and thermodynamic studies, Chem. Eng. J. 155 (2009) 627–636.
[8] S. Liang, X.Y. Guo, N.C. Feng, Q.H. Tian, Isotherms, kinetics and thermodynamic studies of adsorption of Cu^{2+} from aqueous solutions by Mg^{2+}/K^{+} type orange peel adsorbents, J. Hazard. Mater. 174 (2010) 756–762.
[9] S. Wang, H.T. Li, Kinetic modelling and mechanism of dye adsorption on unburned carbon, Dyes Pigments 72 (2007) 308–314.
[10] F.A. Pavan, E.C. Lima, S.L.P. Dias, A.C. Mazzocato, Methylene blue biosorption from aqueous solutions by yellow passion fruit waste, J. Hazard. Mater. 150 (2008) 703–712.
[11] B. Royer, N.F. Cardoso, E.C. Lima, V.S.O. Ruiz, T.R. Macedo, C. Airoldi, Organofunctionalized kenyaite for dye removal from aqueous solution, J. Colloid Interface Sci. 336 (2009) 398–405.
[12] V.K. Gupta, Suhas, Application of low-cost adsorbents for dye removal—a review, J. Environ. Manage. 90 (2009) 2313–2342.
[13] V.B.H. Dang, H.D. Doan, T. Dang-Vu, A. Lohi, Equilibrium and kinetics of biosorption of cadmium(II) and copper(II) ions by wheat straw, Bioresour. Technol. 100 (2009) 211–219.
[14] C.G. Rocha, D.A. Zaia, R.V.S. Alfaya, A.A.S. Alfaya, Use of rice straw as biosorbents for removal of Cu(II), Zn(II) and Hg(II) ions in industrial effluents, J. Hazard. Mater. 166 (2009) 383–388.
[15] A.N. Módenes, J.M.T.A. Pietrobelli, F.R. Espinoza-Quiñones, Cadmium biosorption by non-living aquatic macrophytes *Egeria densa*, Water Sci. Technol. 60 (2009) 293–300.
[16] A.N. Módenes, J.M.T.A. Pietrobelli, F.R. Espinoza-Quiñones, P.Y.R. Suzaki, V.L. Alflen, M.R. Fagundes-Klen, Potencial de biossorção do zinco pela macrófita *egeria densa*, Eng. Sanit Ambient 14 (2009) 465–470.
[17] J.M.T.A. Pietrobelli, A.N. Módenes, M.R. Fagundes-Klen, F.R. Espinoza-Quiñones, Cadmium, copper and zinc biosorption study by non-living *Egeria densa* biomass, water, air, soil, Pollution 202 (2009) 385–392.
[18] C.E. Borba, R. Guirardello, E.A. Silva, M.T. Veit, C.R. Tavares, Removal of nickel(II) ions from aqueous solution by biosorption in a fixed bed column: experimental and theoretical breakthrough curves, Biochem. Eng. J. 30 (2006) 184–191.
[19] O. Karnitz Jr., L.V.A. Gurgel, J.C.P. Melo, V.R. Botaro, T.M.S. Melo, R.P.F. Gil, L.F. Gil, Adsorption of heavy metal ion from aqueous single metal solution by chemically modified sugarcane bagasse, Bioresour. Technol. 98 (2007) 291–1297.
[20] A. Annadurai, R.S. Juang, D.J. Lee, Adsorption of heavy metals from water using banana and orange peel, Water Sci. Technol. 47 (2002) 185–190.
[21] N.C. Feng, X.Y. Guo, S. Liang, Adsorption study of copper(II) by chemically modified orange peel, J. Hazard. Mater. 164 (2009) 1286–1292.
[22] R.P. Dhakal, K.N. Ghimire, K. Inoue, Adsorptive separation of heavy metals from an aquatic environment using orange waste, Hydrometallurgy 79 (2005) 182–190.
[23] S. Liang, X. Guo, N. Feng, Q. Tian, Application of orange peel xanthate for the adsorption of Pb^{2+} from aqueous solutions, J. Hazard. Mater. 170 (2009) 425–429.
[24] Y.S. Ho, Isotherms for the sorption of lead onto peat: comparison of linear and non-linear methods, Polish J. Environ. Stud. 15 (2006) 81–86.
[25] J. Kennedy, R. Eberhart, Swarm Intelligence, Morgan Kaufmann Publishers, San Francisco, CA, 2001.
[26] D.E.G. Trigueros, A.N. Módenes, F.R. Espinoza-Quiñones, A.D. Kroumov, The evaluation of benzene and phenol biodegradation kinetics by applying non-structured models, Water Sci. Technol. 61 (2010) 1289–1298.
[27] D.E.G. Trigueros, A.N. Módenes, A.D. Kroumov, F.R. Espinoza-Quiñones, Modeling of biodegradation process of BTEX compounds: kinetic parameters estimation by using Particle Swarm Global Optimizer, Process Biochem. 45 (2010) 1355–1361.
[28] F.R. Espinoza-Quiñones, A.N. Módenes, L.P. Thomé, S.M. Palácio, D.E.G. Trigueros, A.P. Oliveira, N. Szymanski, Study of the bioaccumulation kinetic of lead by living aquatic macrophyte *Salvinia auriculata*, Chem. Eng. J. 150 (2009) 316–322.
[29] G. Crini, H.N. Peindy, F. Gimbert, C. Robert, Removal of C.I. Basic Green 4 (Malachite Green) from aqueous solutions by adsorption using cyclodextrin-based adsorbent: kinetic and equilibrium studies, Sep. Purif. Technol. 53 (2007) 97–110.
[30] M. Arami, N.Y. Limaee, N.M. Mahmoodi, N.S. Tabrizi, Removal of dyes from colored textile wastewater by orange peel adsorbent: equilibrium and kinetic studies, J. Colloid Interface Sci. 288 (2005) 371–376.
[31] M. Alkan, M. Doğăn, Y. Turhan, Ö. Demirbas, P. Turan, Adsorption kinetics and mechanism of maxilon blue 5G dye on sepiolite from aqueous solutions, Chem. Eng. J. 139 (2008) 213–223.

[32] S. Lagergren, Kungliga Svenska Vetenskapsakademiens, Handlingar 24 (1898) 1.
[33] Y.S. Ho, G. McKay, Trans. IChemE 76 (1998) 183.
[34] Y.S. Ho, Review of second-order models for adsorption systems, J. Hazard. Mater. B136 (2006) 681–689.
[35] W.J. Weber, J.C. Morriss, Kinetics of adsorption on carbon from solution, J. Sanit. Eng. Div. Am. Soc. Civil Eng. 89 (1963) 31–60.
[36] S. Wang, H. Li, L. Xu, Application of zeolite MCM-22 for basic dye removal from wastewater, J. Colloid Interface Sci. 295 (2006) 71–78.
[37] B.H. Hameed, A.A. Ahmad, N. Aziz, Isotherms, kinetics and thermodynamics of acid dye adsorption on activated palm ash, Chem. Eng. J. 133 (2007) 195–203.